

Multi-Dimensional Verification of the Two-Fluid Momentum Equation on Dispersed Flows

Seung-Jun Lee, Byoung Jae Kim*, Ik Kyu Park

Thermal Hydraulics Safety Department, Korea Atomic Energy Research Institute
1045 Daedeok-daero, Yuseong-gu, Daejeon, 305-353, Republic of Korea

*Corresponding author: byoungjae@kaeri.re.kr

1. Introduction

The two-fluid model is widely used in the multi-phase flow analysis. The governing equations are obtained by averaging the local instantaneous conservation equations in time, volume, over ensemble or in some combination of these. Among them, the time[1] and volume[2] averagings have been popularly used in gas-liquid two-phase flows. The standard two-fluid model treats the dispersed phase, such as bubble or mist flow, as a materially-connected phase (continuous phase), and thus there is a difficulty in modeling stress terms in the averaged momentum equations.

Anderson and Jackson[3] and Prosperetti[4] formulated the averaged momentum equations for dispersed flow in a different manner. They averaged the equation of a solid/fluid particle motion that includes various force terms such as the drag, lift, added mass, and history forces. The approach might be more reasonable for dispersed flow. Recently, Kim et al[5, 6] showed theoretically that the different momentum equations can predict the motion of the fluid particle against the surrounding fluid correctly. This approach is validated through one-dimensional simulations in a pipe, contraction and expansion.

In this study the averaged two-fluid momentum equations based on the equation of a fluid particle are investigated with a multi-dimensional thermal hydraulic code, CUPID. The CUPID code has been developed in Korea Atomic Energy Research Institute (KAERI) for the analysis of transient two-phase flows in nuclear reactors. It employs a two-fluid three-field model. The governing equations are discretized by the finite volume method (FVM) and uses unstructured mesh. The validation of CUPID can be found in Yoon's paper[7]. Since CUPID is a multi-dimensional code, it does not need any wall friction partitioning terms used in one dimensional thermal hydraulics codes but solves the shear stress directly. The validity of the momentum equations is checked by solving a simple two-dimensional turbulent channel flow without gravity including the parameter variations, such as inlet velocity, Reynolds number, mesh, inlet void fraction.

2. Two-Fluid Momentum Equations

2.1 Two-Fluid Momentum Equations

The governing equations for the Eulerian-Eulerian approach are obtained by taking the time-[1] and

volume-[2] average over the conservation equations. For adiabatic incompressible flows, the momentum equation for a phase k is given by

$$\begin{aligned} \alpha_k \rho_k \frac{\partial \mathbf{v}_k}{\partial t} + \alpha_k \rho_k \mathbf{v}_k \cdot \nabla \mathbf{v}_k \\ = -\alpha_k \nabla p_k + \nabla \cdot (\alpha_k \boldsymbol{\tau}_k) + \nabla \cdot (\alpha_k \boldsymbol{\tau}_k^{\text{Re}}) + \mathbf{f}_{ik} + \alpha_k \rho_k \mathbf{g} \end{aligned} \quad (1)$$

Meanwhile, Anderson & Jackson[3] derived the momentum equations from the equation of motion for a single solid particle and the Navier-Stokes equation for fluid. If collisions between particles are not taken into account, the momentum equation for a phase k is given by the following modified form as

$$\begin{aligned} \alpha_k \rho_k \frac{\partial \mathbf{v}_k}{\partial t} + \alpha_k \rho_k \mathbf{v}_k \cdot \nabla \mathbf{v}_k \\ = -\alpha_k \nabla p_c + \alpha_k \nabla \cdot \boldsymbol{\tau}_c + \nabla \cdot (\alpha_k \boldsymbol{\tau}_k^{\text{Re}}) + \mathbf{f}_{ik} + \alpha_k \rho_k \mathbf{g} \end{aligned} \quad (2)$$

where the subscript c denotes the continuous-phase. The key difference from Eq. (1) is that the pressure and the viscous stresses of the continuous phase are used for every phases. This is because the motion of the dispersed phase is caused by the stresses of the surrounding continuous fluid. In Eq. (2), α_k is outside of the divergence operator with regard to the viscous stress tensor, whereas it is inside of the divergence operator in Eq. (1). Moreover, as shown in Eq. (2), the disperse-phase equation is expressed with the pressure and viscous stresses of the continuous-phase. Physically, this means that the disperse-phase such as bubbles and droplets move in response to the surrounding continuous fluid. The pressure and stresses inside the disperse-phase are determined by the hydrodynamic relations with surrounding fluid quantities and the interfacial jump conditions.

Following equations show the formulation of the momentum equations in the CUPD code according to the abovementioned theories in Eq. (1) and Eq. (2).

For bubbly flows, the disperse-phase is gas ($d=g$) and the continuous-phase is liquid ($c=f$). The first type in Eq. (1) is applied to Eqs. (3)-(4), and the second type in Eq. (2) is for Eqs. (5)-(6), as follows:

$$\begin{aligned} \alpha_g \rho_g \frac{\partial \mathbf{v}_g}{\partial t} + \alpha_g \rho_g \mathbf{v}_g \cdot \nabla \mathbf{v}_g \\ = -\alpha_g \nabla p + \nabla \cdot (\alpha_g \boldsymbol{\tau}_g) + \nabla \cdot (\alpha_g \boldsymbol{\tau}_g^{\text{Re}}) + \mathbf{f}_i + \alpha_g \rho_g \mathbf{g} \end{aligned} \quad (3)$$

$$\alpha_f \rho_f \frac{\partial \mathbf{v}_f}{\partial t} + \alpha_f \rho_f \mathbf{v}_f \cdot \nabla \mathbf{v}_f = -\alpha_f \nabla p + \nabla \cdot (\alpha_f \boldsymbol{\tau}_f) + \nabla \cdot (\alpha_f \boldsymbol{\tau}_f^{\text{Re}}) - \mathbf{f}_i + \alpha_f \rho_f \mathbf{g} \quad (4)$$

$$\alpha_g \rho_g \frac{\partial \mathbf{v}_g}{\partial t} + \alpha_g \rho_g \mathbf{v}_g \cdot \nabla \mathbf{v}_g = -\alpha_g \nabla p + \alpha_g \nabla \cdot \boldsymbol{\tau} + \nabla \cdot (\alpha_g \boldsymbol{\tau}_g^{\text{Re}}) + \mathbf{f}_i + \alpha_g \rho_g \mathbf{g} \quad (5)$$

$$\alpha_f \rho_f \frac{\partial \mathbf{v}_f}{\partial t} + \alpha_f \rho_f \mathbf{v}_f \cdot \nabla \mathbf{v}_f = -\alpha_f \nabla p + \alpha_f \nabla \cdot \boldsymbol{\tau} + \nabla \cdot (\alpha_f \boldsymbol{\tau}_f^{\text{Re}}) - \mathbf{f}_i + \alpha_f \rho_f \mathbf{g} \quad (6)$$

where \mathbf{f}_i is the substitution of \mathbf{f}_{ik} in Eq. (1). Given the absence of phase change, the interfacial jump condition for momentum leads to $\mathbf{f}_{if} = -\mathbf{f}_{ig} = -\mathbf{f}_i$. In Eqs. (3) to (6), a single pressure is assumed; $p = p_g = p_f$. For incompressible flows, the viscous stress terms are expressed as $\boldsymbol{\tau}_g = \mu_g \nabla \mathbf{v}_g$ and $\boldsymbol{\tau}_f = \mu_f \nabla \mathbf{v}_f$.

2.2 Turbulence Model

The standard $k - \varepsilon$ transport equations are solved to obtain k_f (turbulence kinetic energy) and ε_f (viscous dissipation rate). The constants have been obtained through comprehensive data fitting for a wide range of turbulent flows[8]: $C_\mu = 0.09$, $\sigma_k = 1.0$, $\sigma_\varepsilon = 1.4$, $C_{\varepsilon 1} = 1.44$, and $C_{\varepsilon 2} = 1.92$. The shear production term is given by $P_f = \mu_f^T \nabla \mathbf{v}_f$. The Reynolds stress of the gas phase is calculated as

$$\frac{\partial(\alpha_f \rho_f k_f)}{\partial t} + \nabla \cdot (\alpha_f \rho_f k_f \mathbf{v}_f) = \nabla \cdot \left[\alpha_f \left(\mu_f + \frac{\mu_f^T}{\sigma_k} \nabla k_f \right) \right] + \alpha_f P_f - \alpha_f \rho_f \varepsilon_f \quad (7)$$

$$\frac{\partial(\alpha_f \rho_f \varepsilon_f)}{\partial t} + \nabla \cdot (\alpha_f \rho_f \varepsilon_f \mathbf{v}_f) = \nabla \cdot \left[\alpha_f \left(\mu_f + \frac{\mu_f^T}{\sigma_\varepsilon} \nabla \varepsilon_f \right) \right] + \frac{\alpha_f \varepsilon_f}{k_f} (C_{\varepsilon 1} P_f - C_{\varepsilon 2} \rho_f \varepsilon_f) \quad (8)$$

For the turbulent shear stress, liquid (or gas) shear-induced turbulence (μ_f^T, μ_g^T) model is used. The kinematic turbulence viscosities of gas and liquid are assumed to be equal[8].

$$\boldsymbol{\tau}_k^{\text{Re}} = \mu_k^T \nabla \mathbf{v}_k, \quad (9)$$

$$\mu_f^T = C_\mu \rho_f k_f^2 / \varepsilon_f, \quad (10)$$

$$\mu_g^T = \mu_f^T \frac{\rho_g}{\rho_f}, \quad (11)$$

2.3 Interfacial Momentum Transfer

The interfacial momentum transfer term, \mathbf{f}_i is used a simple model of Ishii[9] and Yoneda[10].

$$\mathbf{f}_i = \frac{1}{8} A_i \rho_g C_D |\bar{u}_g - \bar{u}_i| (\bar{u}_g - \bar{u}_i), \quad (12)$$

where the interfacial drag coefficients C_D are defined by Ishii[9] for the bubbly flows. To define the Reynolds number, Yoneda[10] model is applied for the Sauter mean diameter.

3. Simulation

3.1 Problem Definition

Figure 1 shows a channel flow in two dimensions. Flow goes into the pipe from the lower part and goes out of the pipe through the upper part as presented in Fig. 1. The other faces of the pipe are closed by walls. No gravity condition is assumed. The pipe has 0.02 m width and 1.00 m height geometry.

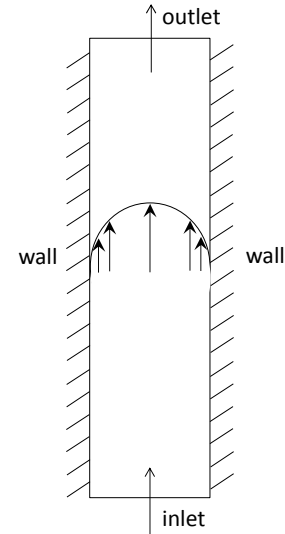


Fig. 1. Turbulent flow in a two-dimensional channel.

Table I contains the test cases to show the validity of the governing equations. All test conditions are based on two-phase water under 0.5 MPa, saturated temperature and 5 % void fraction. Three test cases are defined by the Reynolds numbers. According to the Reynolds number, the inlet velocity condition is calculated as presented in Table I. The standard $k - \varepsilon$ turbulence model is used.

Table I: Test Matrix

	case1	case2	case3
Pressure	0.5 MPa	0.5 MPa	0.5 MPa
Temperature	Saturated	Saturated	Saturated
Re	1000	13600	70000
y+	-	57	216
Inlet α_g	0.05	0.05	0.05
Inlet Velocity	0.00984	0.1338	0.6886
Turbulence	-	k- ε	k- ε

3.2 Results

Figure 2 shows the velocity distribution at outlet for case1 ($Re=1000$). Because the geometry is sufficiently long, the velocity distribution shows fully developed flow. Fig. 2a is the result of the conventional two-fluid momentum equation, which solves the dispersed phase as continuous matter. In Fig. 2a, the gas velocity (V_g) is faster than the liquid velocity (V_l). Physically this result is incorrect. Without gravity and the other turbulent viscous forces, there is no reason to make gas flows faster than liquid in this horizontal pipe. Figure 2b show the results of Eq. (5)~(6). Velocities of gas and liquid became identical.

Figure 3 shows the velocity distribution at outlet for case2 ($Re=13600$). Because the flow is turbulent, $k-\epsilon$ model is applied with the wall function. Fig. 3a is the result of the conventional two-fluid momentum equation. In Fig. 3a, the gas velocity (V_g) is faster than the liquid velocity (V_l). Figure 3b show the results of Eq. (5)~(6). In this case, the velocity of gas phase is still faster since Reynolds viscous stress is influencing on the velocity.

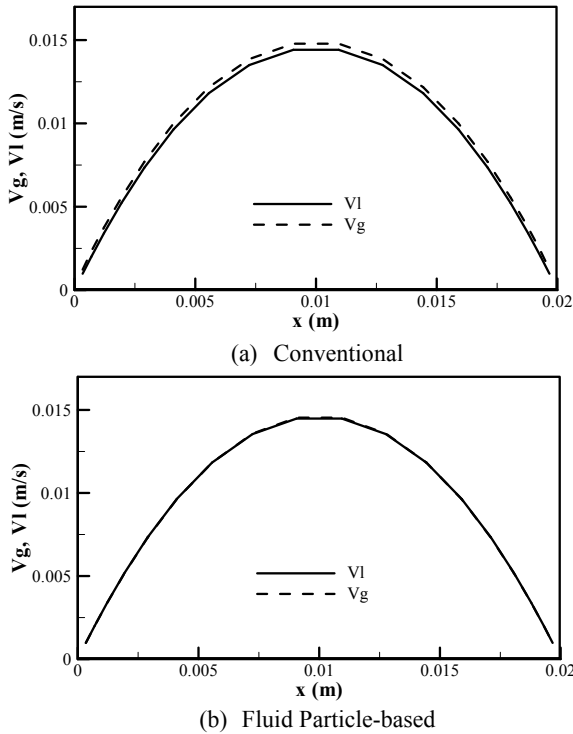


Fig. 2. Velocity distribution for case1.

Figure 4 shows the velocity distribution at outlet for case3 ($Re=70000$). Likewise Fig. 2, the $k-\epsilon$ model is used for case3, Figure 4a is the result of the conventional two-fluid momentum equation. In Fig. 4a and 4b, the gas velocity (V_g) is faster than the liquid velocity (V_l).

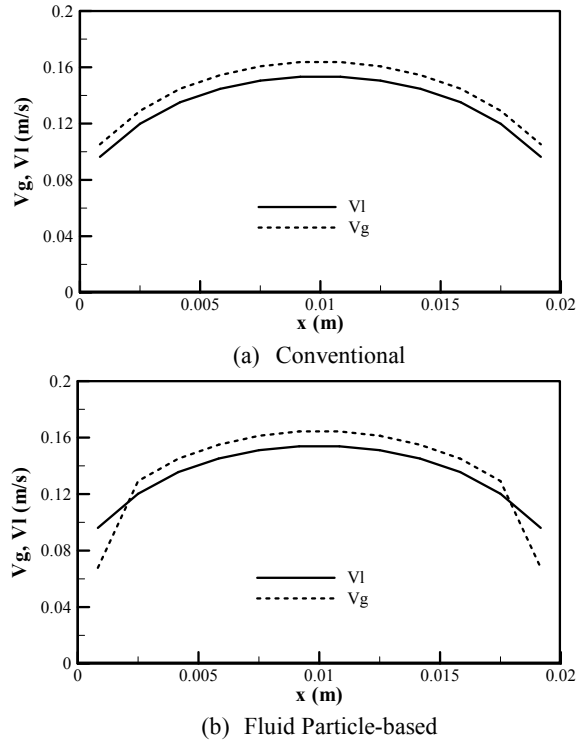


Fig. 3. Velocity distribution for case2.

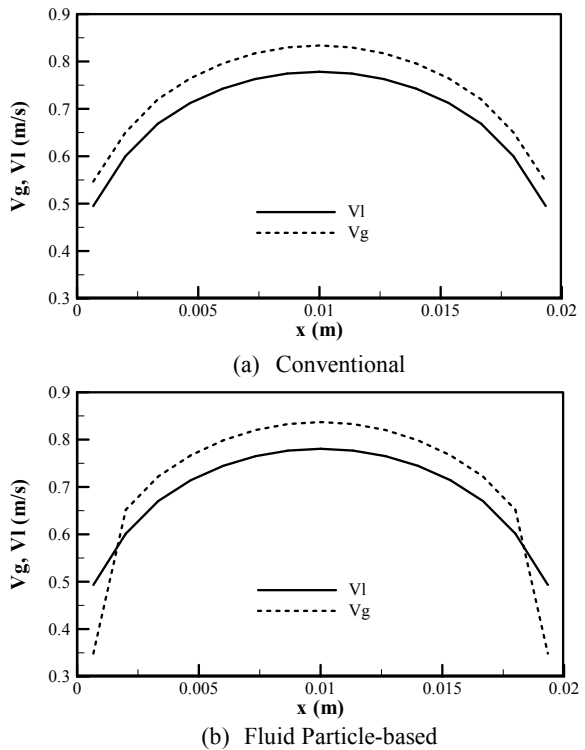


Fig. 4. Velocity distribution for case3.

3.3 Discussion on the velocity difference

In Fig.2, the result from the fluid particle-based approach shows the identical velocity profile between the liquid and gas phase. This is the effect of viscous shear stress apportioned from the background field (here it is the liquid field). In this case the Reynolds stress is

zero. However, Figs. 3-4 show different velocity profiles even when the fluid particle-based two-fluid momentum equation owing to the Reynolds stress effect. Because the Reynolds stress term is originated from the convective term, it cannot be erased as the viscous shear stress is erased in the fluid particle-based derivation. This result is different from the result of the one-dimensional two-fluid momentum equation based on the fluid particle-based derivation, in which the Reynolds stress term is modeled as the viscous shear stress model so that the velocity profiles became identical in turbulent flow cases.

As for the Reynolds stress term, it is also a modeled force. Thus, the term can be modified to correct the velocity profiles to be identical by modeling. For the modeling, the Reynolds stress term can be treated as the viscous shear stress.

3. Conclusions

In this study, the conventional and fluid particle-based two-fluid momentum equation were investigated with the multi-dimensional two-phase code, CUPID. The conventional two-fluid momentum which assumes the shear forces of the dispersed phase as the matter of continuum showed unphysical momentum increase on disperse phase. This issue in laminar flow cases was solved by the modified momentum equation which uses the shear forces as the form of the partitioned viscous force of surrounding fluid according to void fraction of each phase. Furthermore, turbulent cases are tested and the results are different from the one-dimensional approaches in which the Reynolds viscous stress is expressed in terms of the laminar viscosity. Consequently, in solving two-fluid momentum equation, the fluid particle-based form cannot correct the disperse field to be identical. Finally, a model for the Reynolds stress is suggested.

ACKNOWLEDGMENT

This work was supported by the National Research Foundation of Korea (NRF) and the Korea Radiation Safety Foundation (KORSAFe) grant funded by the Korean government (MSIP & NSSC) (Nuclear Research and Development Program: 2012M2A8A4025647, Nuclear Safety Research Center Program: 1305011).

REFERENCES

- [1] M. Ishii, *Thermo-Fluid Dynamic Theory of Two-Phase Flow*, Paris, France: Eyrolles. 1975.
- [2] D.A. Drew, "Mathematical Modeling of Two-Phase Flow," *Annual Review of Fluid Mechanics*, **15**, 261-291 1983.
- [3] T.B. Anderson, R. Jackson, "Fluid Mechanical Description of Fluidized Beds: Equations of Motion," *Industrial & Engineering Chemistry Fundamentals*, **6**, 527-539, 1967.

[4] A. Prosperetti and G Tryggvason, *Averaged Equations for Multiphase Flow in Computational methods for multiphase flow*, 237-281, Yew York, USA: Cambridge University Press, 2007.

[5] B.J. Kim, J. Kim, K.D. Kim, "On the wall drag term in the averaged momentum equation for dispersed flows," *Nuclear Science and Engineering*, **178**, 1-15, 2014.

[6] B.J Kim, S.W. Lee, K.D. Kim, "New wall drag and form loss models for one dimensional dispersed two-phase flow," *Submitted to Nuclear Science and Technology*, accepted for publication.

[7] H.Y. Yoon, H.K. Cho, J.R. Lee, I.K. Park and J.J. Jeong, "Multi-scale thermal hydraulic analysis of PWRs using the CUPID code," *Nuclear Engineering and Technology*, **44**, 8, 831-846, 2012.

[8] Y. Sato, K. Sekoguchi, "Liquid velocity distribution in two-phase bubble flow," *International Journal of Multiphase Flow*, **2**, 79-95, 1975.

[9] M. Ishii, T. Hibiki, *Thermo-Fluid Dynamics of Two-Phase Flow*, 2nd Edition, Springer, 2011.

[10] K. Yoneda, T. Okawa, A. Yasuo, "Structure of steam-water two-phase flow in a vertical pipe," Proc. Of 6th Int. Conf. on Nuclear Engineering (ICONE-6), San Diego, 6361, 1998.